

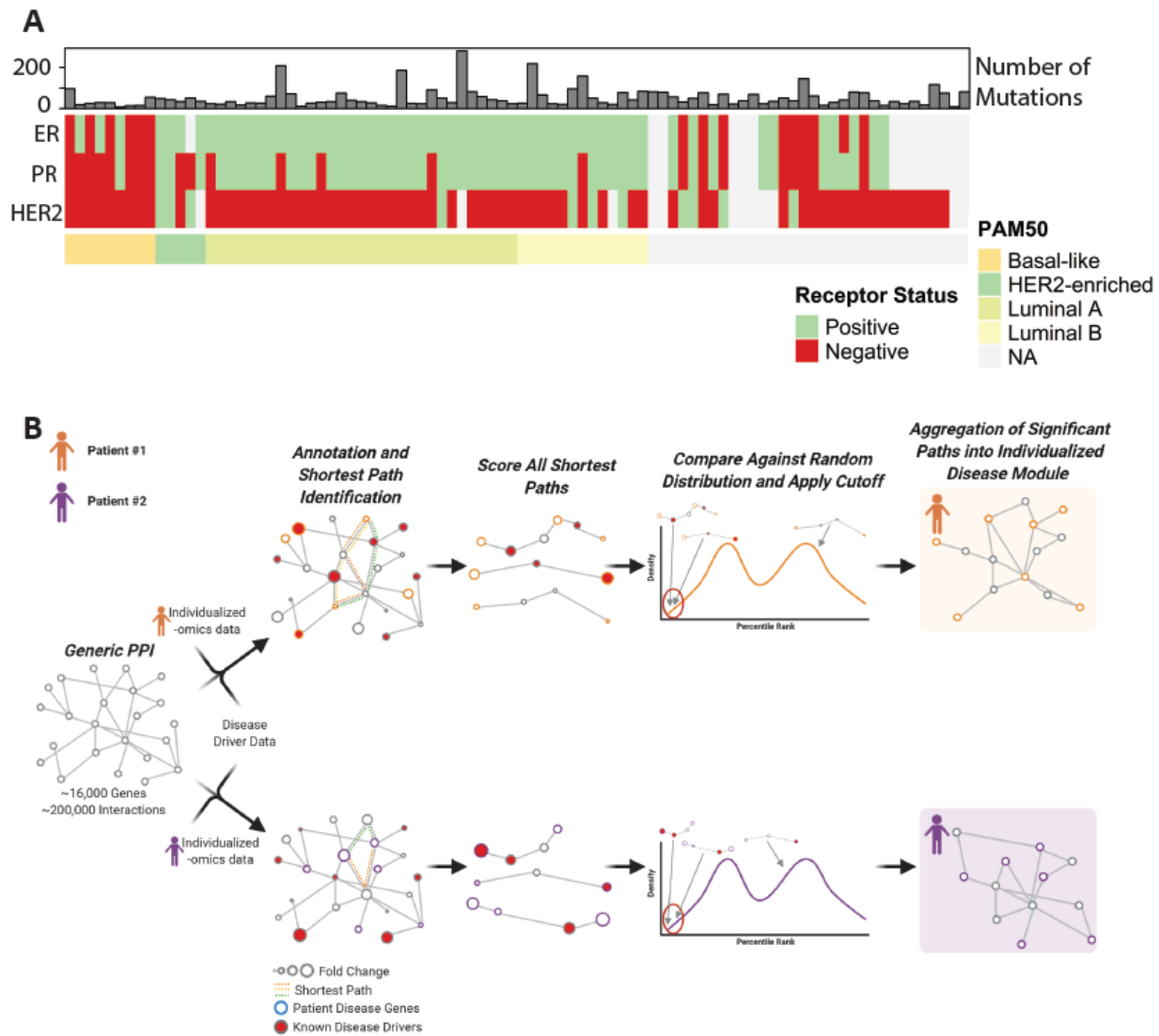
Supplemental Figures S1-S12**De novo individualized disease modules reveal the synthetic penetrance of genes and inform personalized treatment regimens****Authors**

Taylor M. Weiskittel¹, Choong Y. Ung¹, Cristina Correia¹, Cheng Zhang¹, and Hu Li^{1*}

Affiliations

1. Center for Individualized Medicine, Department of Molecular Pharmacology and Experimental Therapeutics, Mayo Clinic College of Medicine, Rochester, MN 55905, USA.

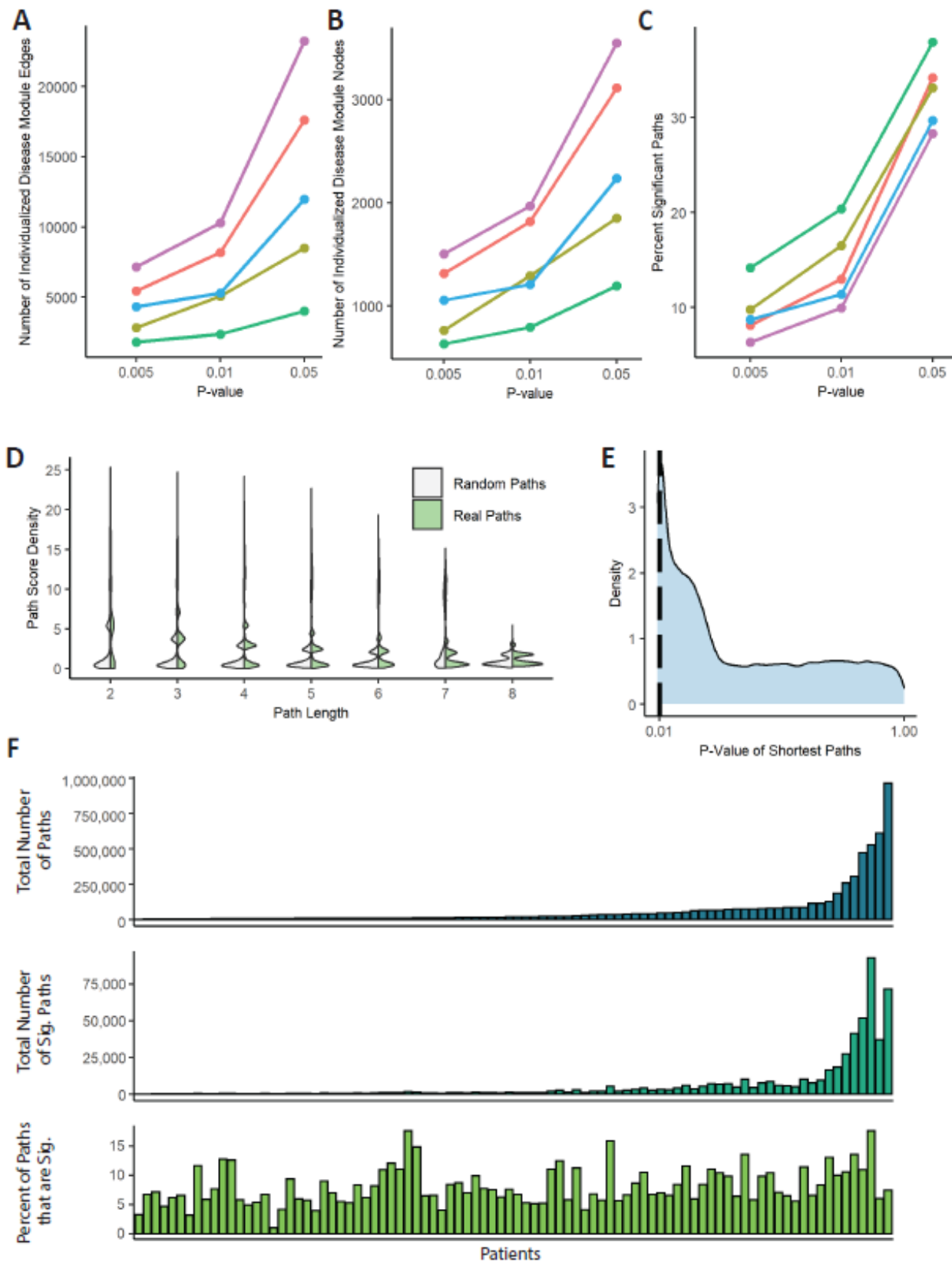
* Correspondence to: li.hu@mayo.edu



Supplemental Figure 1. Clinical characteristics of Breast Cancer cohort patients used in this study and extended network construction schematics.

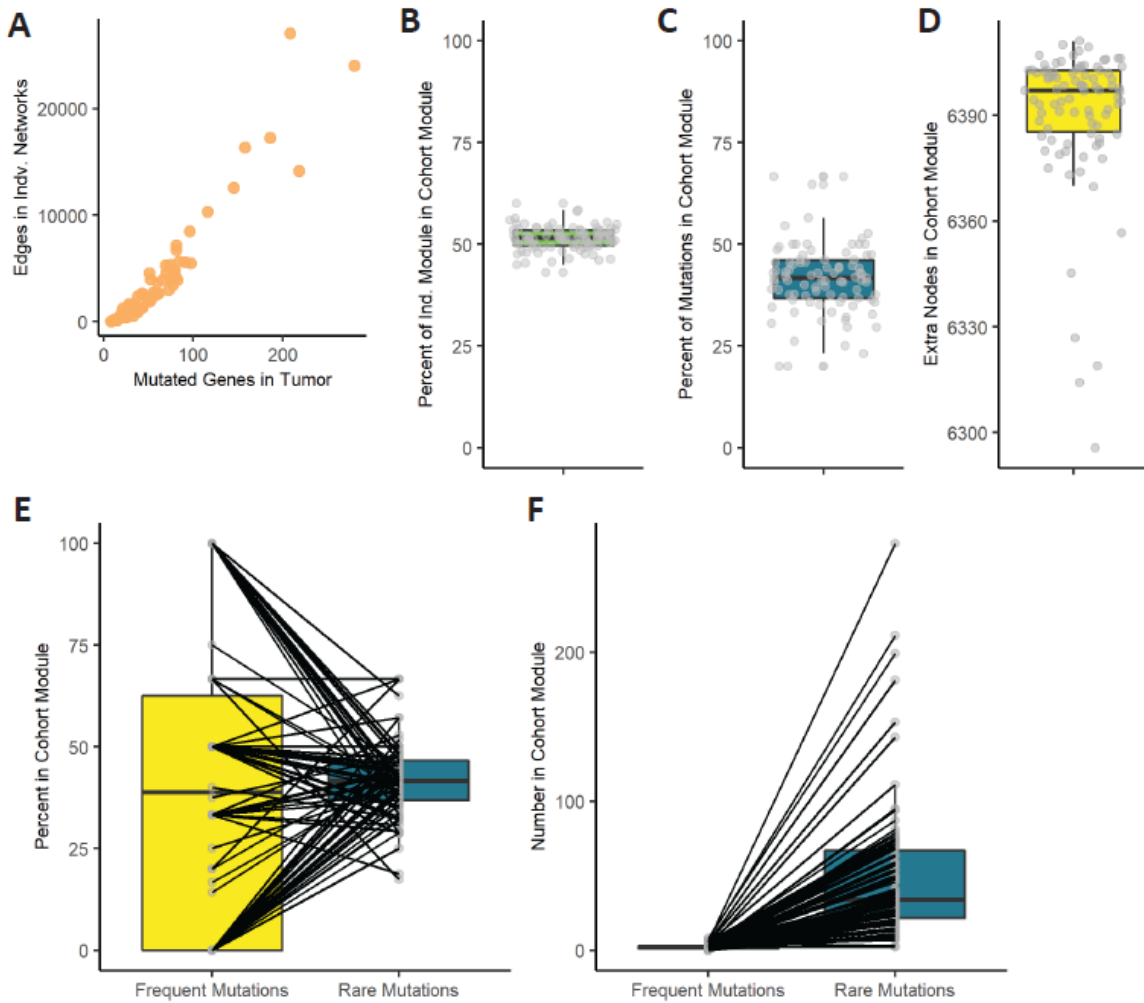
A) Heatmap describing the characteristics of the cohort's breast cancer tumors. The heatmap body shows hormone receptor (ER, PR and HER2) status as positive (green), negative (red), or not accessed (NA). PAM50 subtypes are documented by the bottom annotation, and the number of mutated genes in each patient is shown in the top histogram (available from TCGA BRCA project).

B) Extended network construction schematics showing how network construction differs for two separate hypothetical patients #1 and #2.



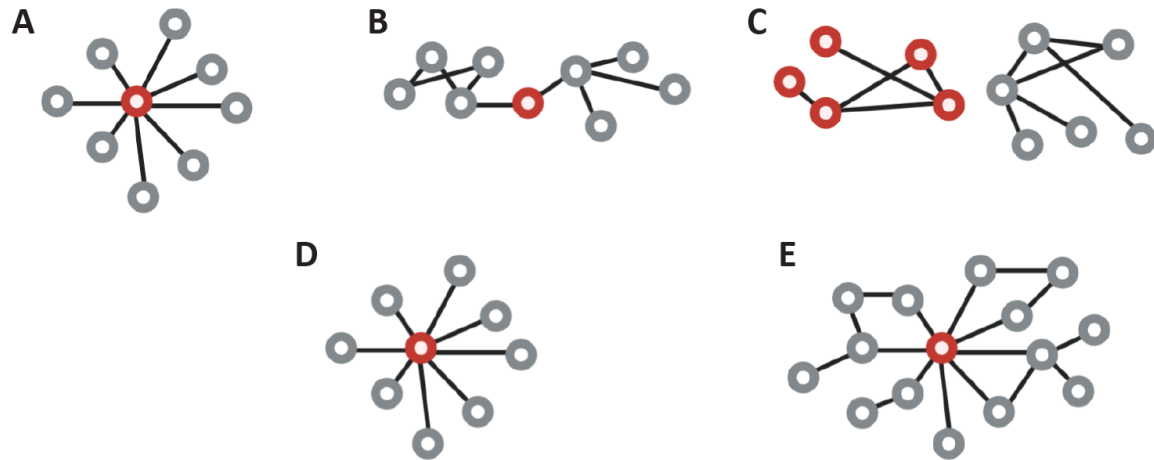
Supplemental Figure 2. Characterization of path scoring and empirical p-value cutoffs.

Plots showing edge number **A**), node number **B**), and significant path percentages **C**) of the individualized disease modules of five patients subjected to three different p-value cut-offs (0.005, 0.01, and 0.05). **D**) Violin plots showing all patient path scores as density plots for random and real paths separated by path length. **E**) Density plot of all cohort empirical p-values combined. **F**) Bar charts displaying the total number of paths (top), the number of significant paths (middle), and the percent of paths that were considered significant (bottom) for each patient for a p-value <0.01 . Each patient is represented by the vertically aligned columns across the three plots.



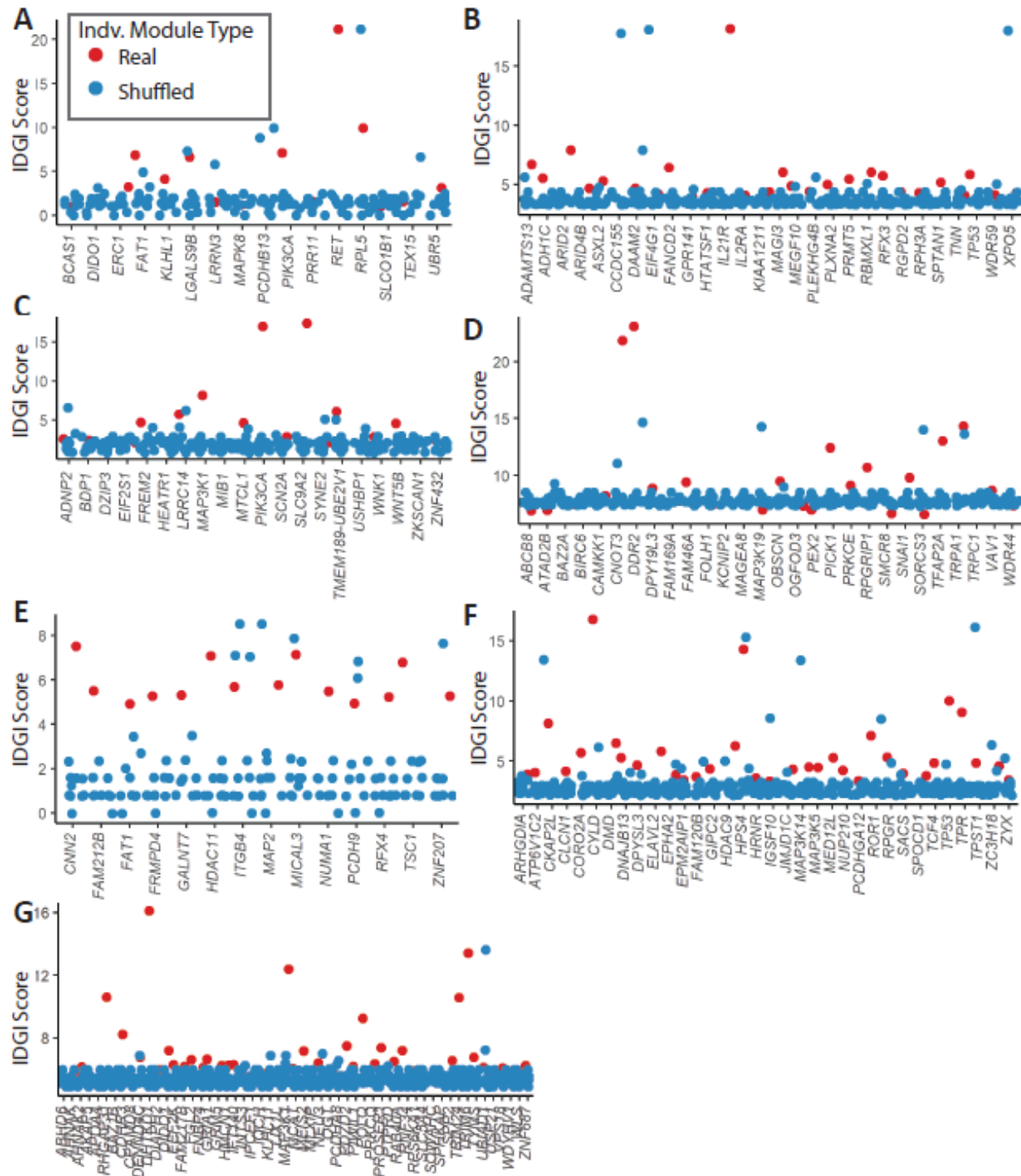
Supplemental Figure 3. Individualized disease module characteristics and comparisons to cohort disease modules.

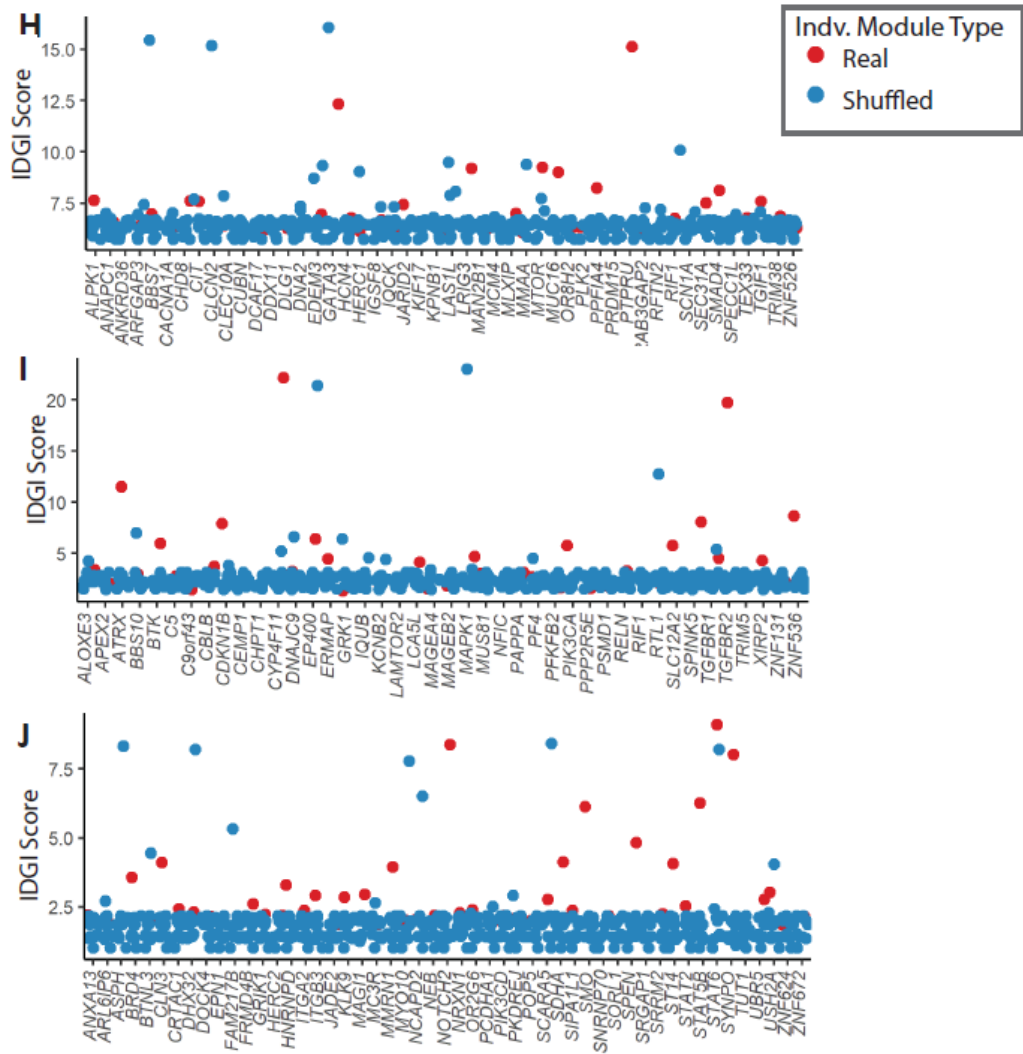
A) Scatter plot of the number of edges in the individualized disease networks versus the number of mutated genes in the tumor. **B-C)** The percent of individualized disease module nodes **B)** and mutations **C)** included in the cohort disease module. **D)** The number of nodes present in the cohort disease module that were not represented in individualized disease modules. **E-F)** The percentage **E)** and absolute number **F)** of frequent ($\geq 5\%$ of the TCGA BRCA cohort) and rare ($< 5\%$ of TCGA BRCA cohort) mutations present in the cohort module.



Supplemental Figure 4. Schematic showing network components for IDGI score definition.

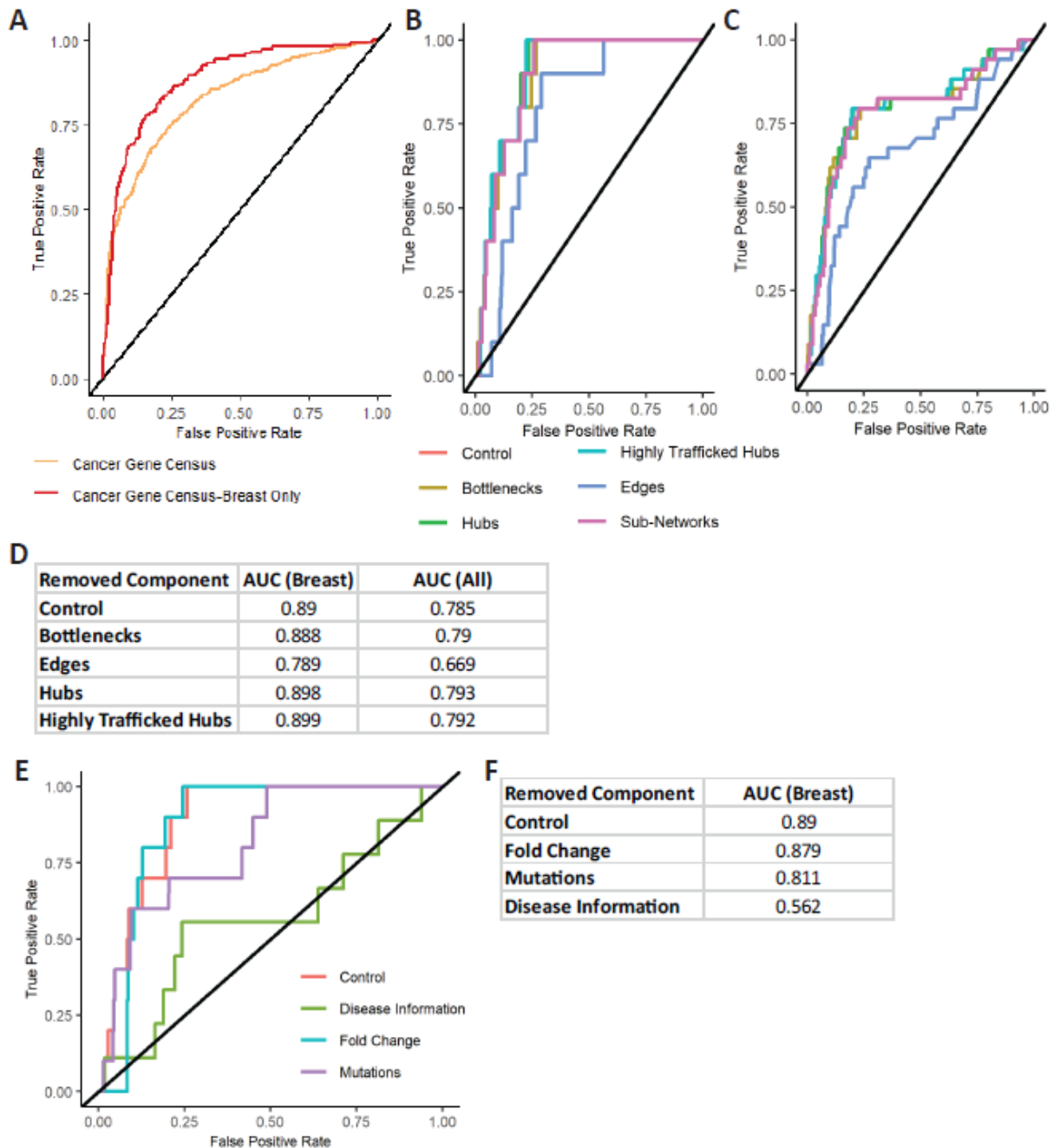
*Schematics demonstrating IDGI scoring components including **A**) hubs, **B**) bottlenecks, **C**) separate network components, **D**) lowly trafficked hubs, and **E**) highly trafficked hubs.*





Supplemental Figure 5. Randomized validation of IDGI scores showing relevance of real scores.

A-J) Dot plots for patients ($n=10$) that underwent randomized shuffle validations. Shuffled scores are shown in blue, and real scores are shown in red.



Supplemental Figure 6. IDGI score for detection of known cancer drivers and ablation studies showing importance of score components.

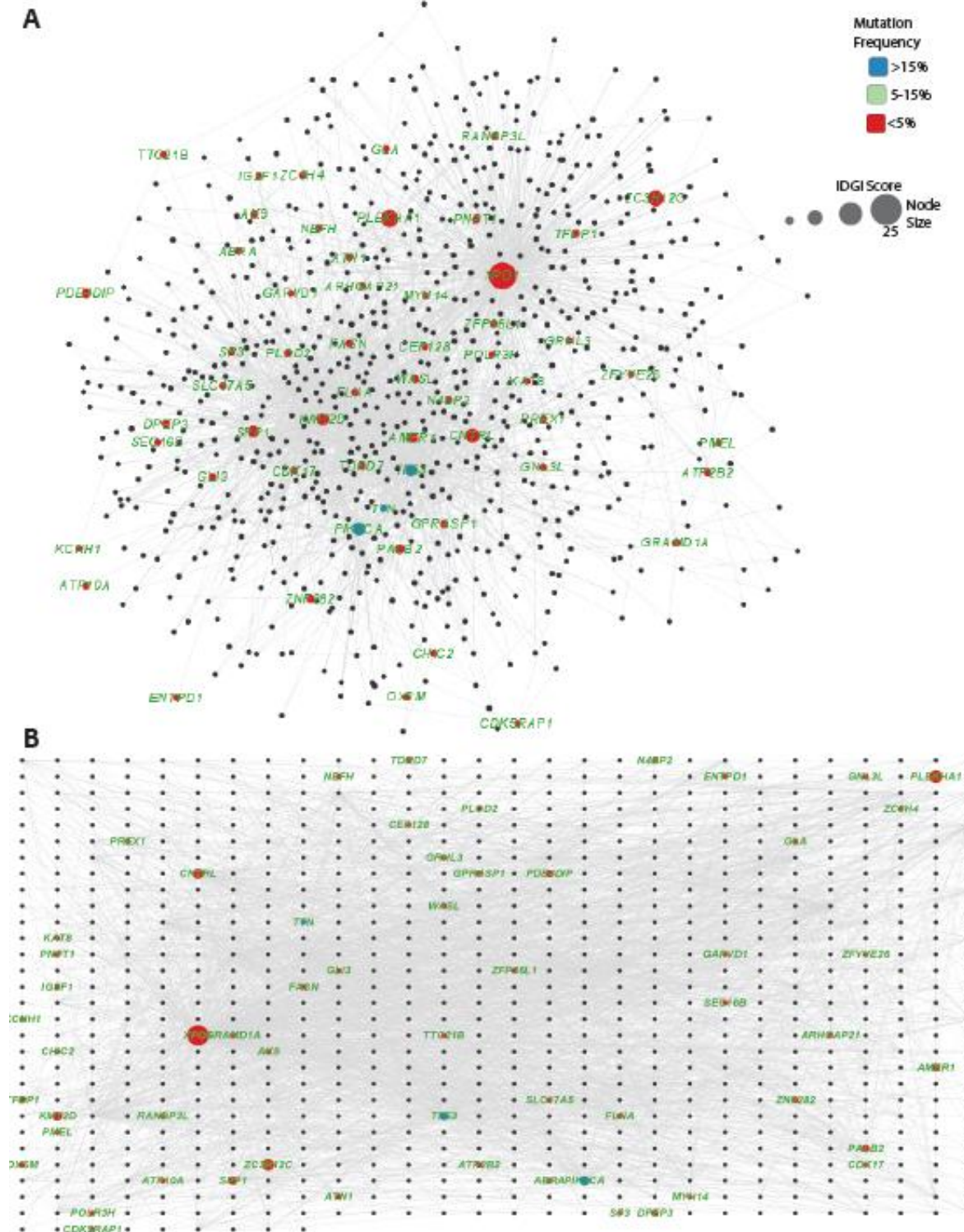
A) Receiver operating characteristic (ROC) curve for cooperativity score recovery of Cancer Gene Census (CGC genes) for all cancers (orange) or breast cancers (red). B-C) ROC curve for

*recovery of CGC **B**) breast cancer genes and **C**) all cancer genes with individual gene score components deleted. **D**) AUC values for the ROC curves shown in panels **S6B** and **S6C**. **E**) Receiver operating characteristic (ROC) curves for the ablation of each path score component compared to the control (no ablation), and its ability to recover breast cancer genes in the CGC. **F**) AUC values for the ROC curve in **S6E**.*



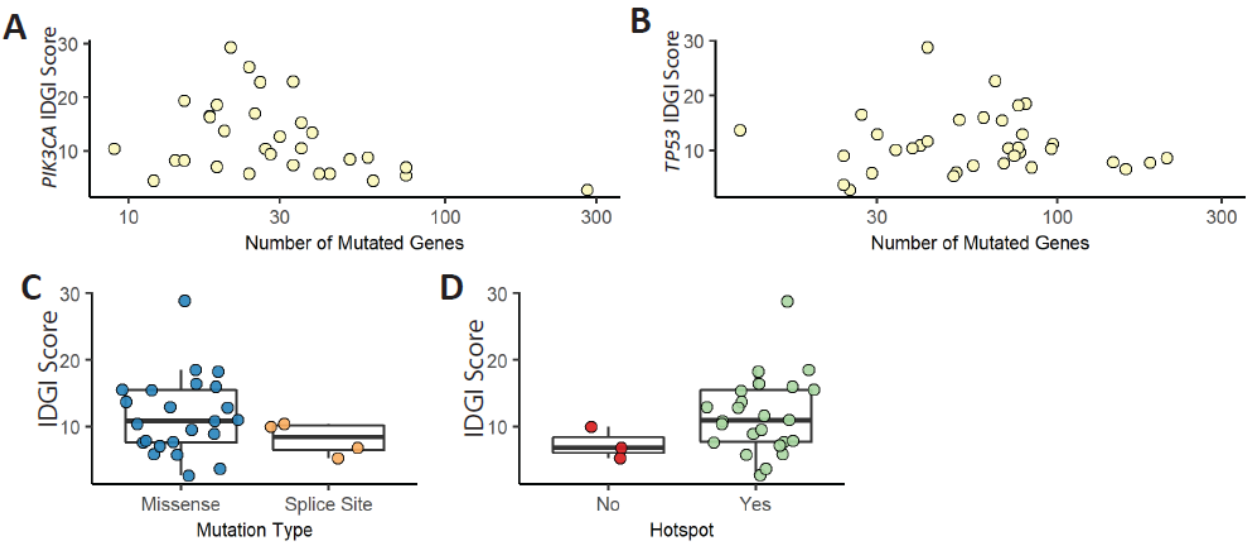
Supplemental Figure 7. Full individualized disease modules.

A-B) Full disease module for patient shown in **Figure 3A** shown in **A)** network and **B)** grid view.



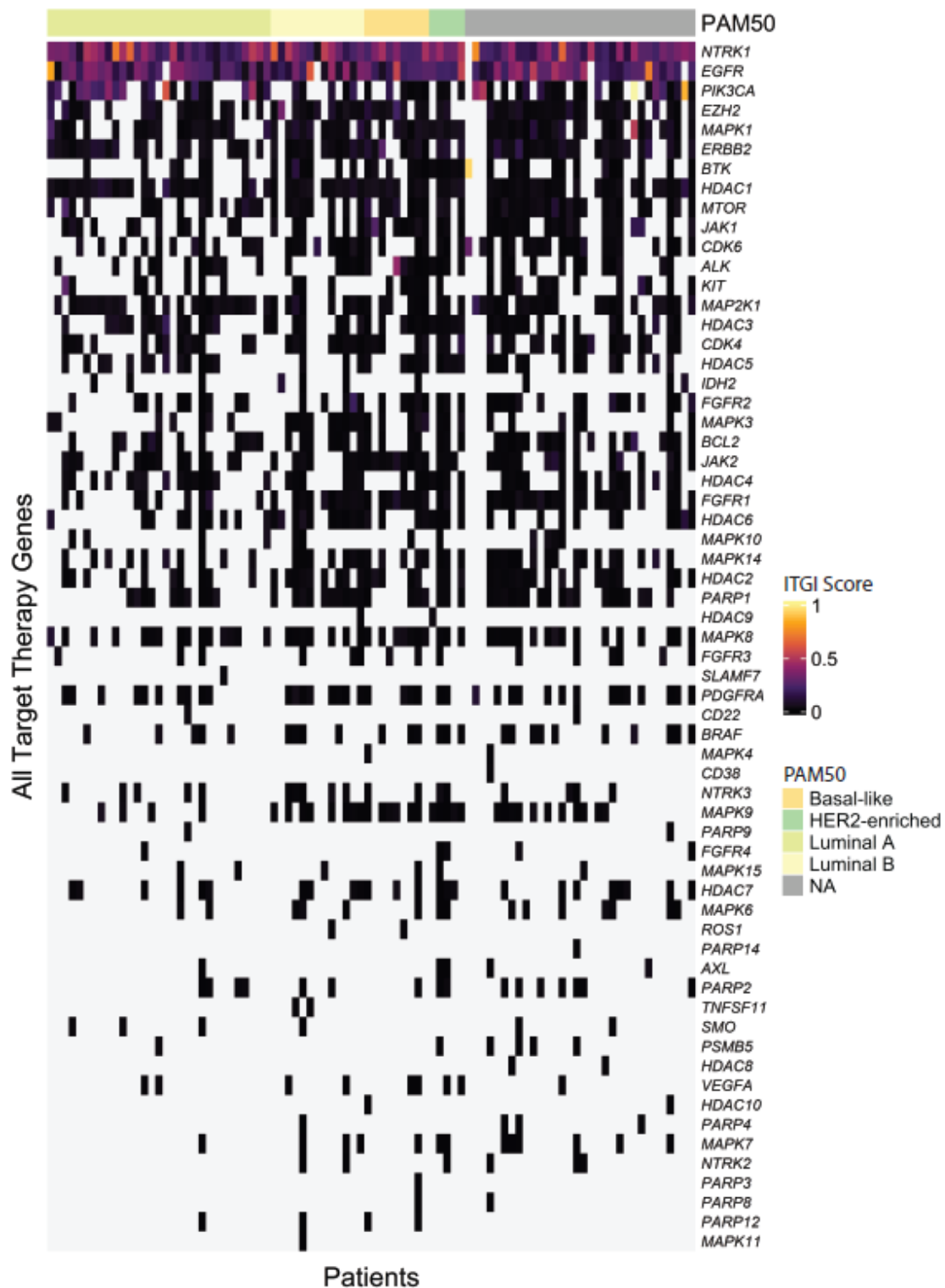
Supplemental Figure 8. Full individualized disease modules.

A-B) Full disease module for patient shown in **Figure 3B** shown in a **A)** network and **B)** grid view.



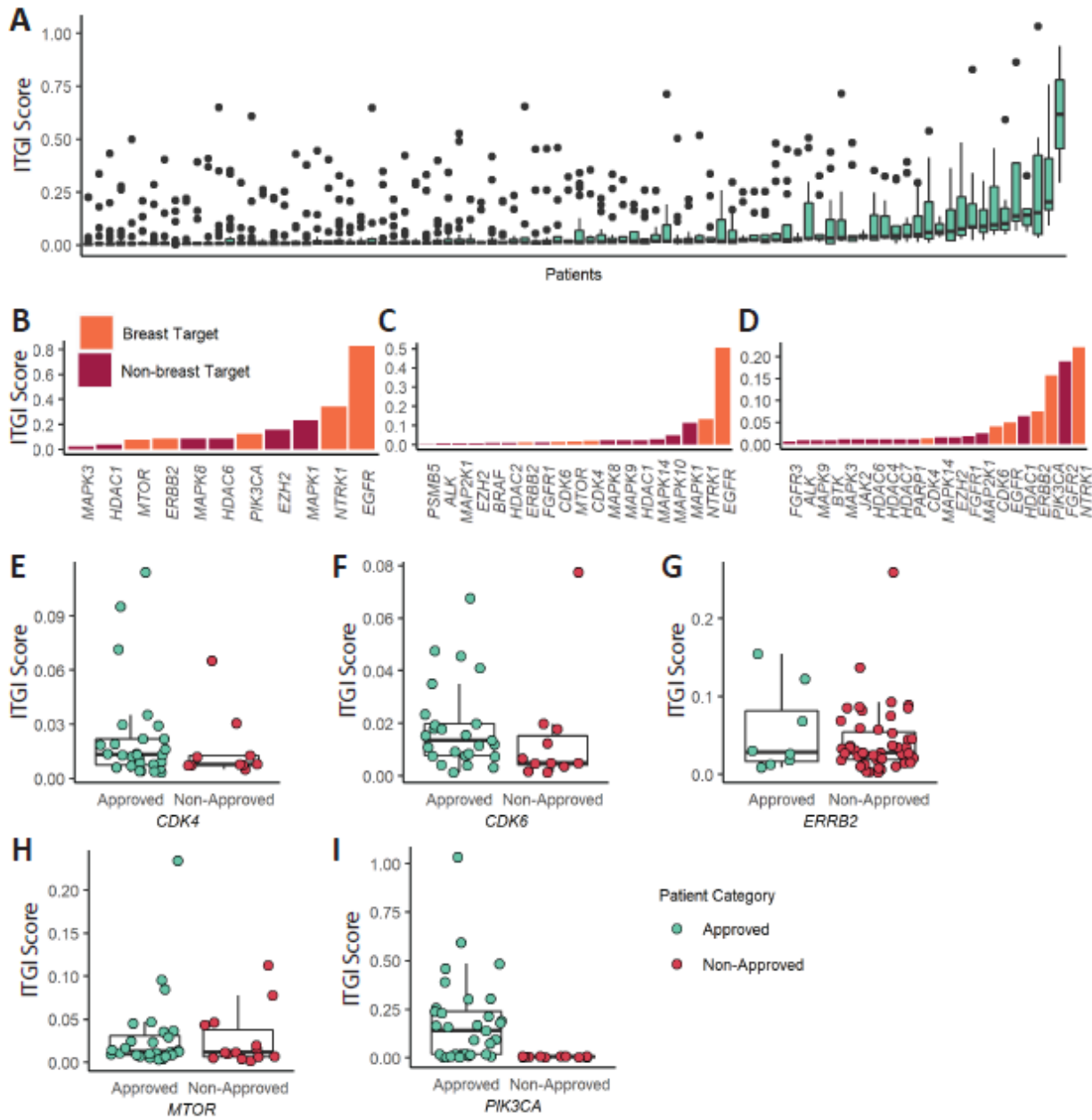
Supplemental Figure 9. Gene importance relates to biological properties.

A) and **B)** IDGI scores for TP53 and PIK3CA mutations versus the number of mutations within that tumor. **C)** IDGI score boxplots for missense and splice site TP53 mutations. **D)** IDGI score boxplots for TP53 missense mutations within and outside of mutational hotspots.



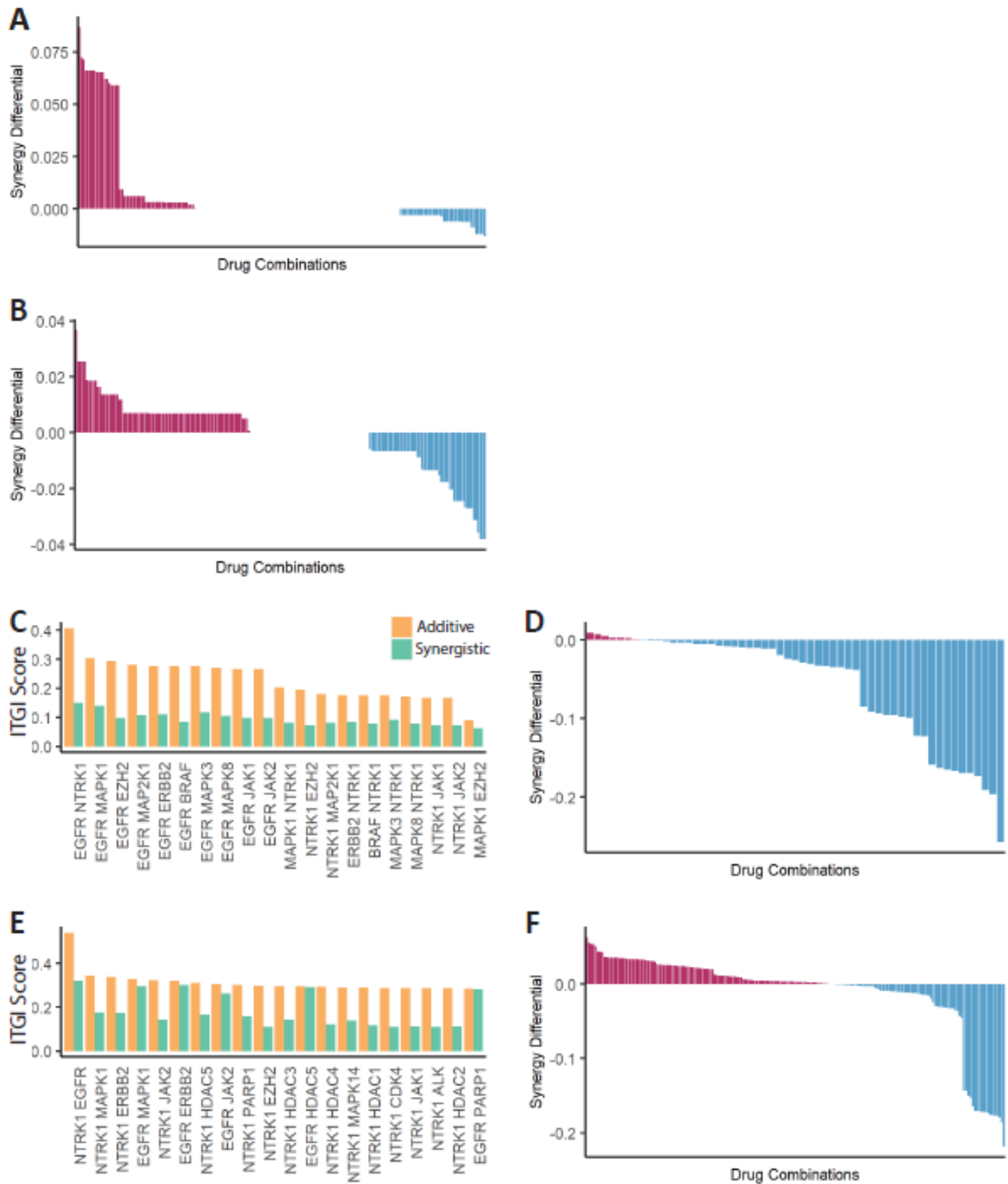
Supplemental Figure 10. Diversity of targeted therapy responses.

Extended heatmap showing ITGI scoring for all target therapy genes in all BC patients.



Supplemental Figure 11. Individualized therapeutic target prioritization with individual network destabilization.

A) Boxplots showing target score across each cohort patient. **B-D)** Target scoring for individual patients. **E-I)** Targeting score for targets approved for a subset of breast cancer patients show by approved patients (green) and non-approved patients (red). Approval indications are documented in **Data S1**.



Supplemental Figure 12. Synergistic and redundant combinatorial targeting across several patients.

A-B) Additional representative drug synergy differential (synergistic - additive). **C) and E)** Bar plots showing the top combinations of patients with redundant targeting. **D) and F)** Drug synergy differential for these patient's therapeutic combinations.